Correction: page 3

SCATTERING OF FLEXURAL WAVES ON THIN PLATES

A. N. NORRIS AND C. VEMULA

Department of Mechanical and Aerospace Engineering, Rutgers University, Piscataway, New Jersey 08855-0909, U.S.A.

(Received 21 August 1993, and in final form 28 December 1993)

Some general results are presented concerning the scattering of flexural waves from regions of inhomogeneity on flat plates. We derive a flux conservation relation for arbitrary motion, and show that it simplifies for periodic motion. An optical theorem is obtained relating the total scattered flux for a straight-crested incident wave to the scattering amplitude in the forward direction. Scattering by circular inclusions with different plate properties is discussed, and numerical results are presented. The response simplifies for the limiting cases of a hole and a rigid obstacle, but with quite different behavior for each. A rigid obstacle can produce an unbounded scattering cross-section as the frequency tends to zero, whereas the cross-section of a hole vanishes in the same limit.

1. INTRODUCTION

The theory describing flexural or bending motion of flat thin plates is well established, with many excellent books and monographs [1–4]. Most applications are for plates with specified boundary conditions at the edges, and are best attacked using modal summation techniques in both the time and frequency domains. Heterogeneity in the plate, caused by variations in thickness, for example, leads to complications in determining the modes of the system, but they can still be found, in general, by suitable numerical methods. The heterogeneity basically alters the modes, due to wave interactions between the heterogeneity and the boundary. An alternative, and possibly simpler, point of view is to ignore edge effects as a first approximation. This approach is suitable for large plates with distant edges, and leads to much simplification. Thus, canonical solutions, such as the dynamic response of an infinite plate due to point forces and moments [4, 5], are useful building blocks for attacking more realistic problems. In the same manner, we can consider the heterogeneity as interacting with the *waves* on the plate rather than the modes. A compact region of heterogeneity in an otherwise uniform plate therefore acts as a scatterer of waves.

There has been some recent interest in analyzing vibration problems from the scattering point of view [6–8]. Leviatan *et al.* [8] proposed representing the scattered response of a compact region by a superposition of point sources or images. Lapin [7] considered a scattering problem within the context of exact elasticity theory for plates. In this paper, we derive some basic results concerning scattering of flexural waves within the context of classical plate theory. The ideas of energy flux and scattering cross-sections are discussed for arbitrary scatterers. In particular, we derive an optical theorem for flexural waves. The optical theorem is a well-known result in acoustics and electromagnetic wave theory [9–12] which relates the forward scattered amplitude to the total energy scattered, or to the total cross-section. It serves as a useful numerical check on computational results. The latter part of the paper is devoted to scattering by a cylindrical heterogeneity—probably the

simplest possible configuration. The general solution is developed and related to the limiting cases of a rigid inclusion and a hole.

2. ENERGY AND FLUX IDENTITIES

2.1. EQUATIONS OF MOTION

The equations for bending of plates are well known and can be found in many textbooks, such as that of Timoshenko [1]. The displacement is w = w(x, y, t) in the z-direction. For a given direction \mathbf{n} , $|\mathbf{n}| = 1$, with s designating the direction perpendicular to \mathbf{n} , the bending and twisting moments are

$$M_{n} = -D\left(\frac{\partial^{2} w}{\partial n^{2}} + v \frac{\partial^{2} w}{\partial s^{2}}\right), \qquad M_{ns} = D(1 - v) \frac{\partial^{2} w}{\partial n \partial s}, \tag{1}$$

where $D = Eh^3/12(1 - v^2)$, and E and v are the Young's modulus and the Poisson ratio, respectively. The generalized Kirchhoff stress associated with the **n**-direction, V_n , is a combination of the shear stress Q_n and the twisting moment [1, 3],

$$V_n = Q_n - \frac{\partial M_{ns}}{\partial s} = \frac{\partial M_n}{\partial n} - 2 \frac{\partial M_{ns}}{\partial s}.$$
 (2)

The equation of motion for the plate is

$$D\Delta^2 w + \rho h \frac{\partial^2 w}{\partial t^2} = q(\mathbf{x}, t), \tag{3}$$

where $\rho(x)$ is the density per unit volume, h is the thickness, and q is the applied load or pressure.

2.2. ENERGY FLUX CONSERVATION

We now derive some general expressions related to energy flux for bending waves. The point-wise expression of conservation of mechanical energy, in the absence of an external source, can be written

$$\partial U/\partial t + \mathbf{\nabla} \cdot \mathbf{F} = 0, \tag{4}$$

where U is the total strain energy density (per unit area) and \mathbf{F} is the energy flux vector. We have [2]

$$U = \frac{D}{2} \left\{ (\Delta w)^2 - 2(1 - v) \left[\frac{\partial^2 w}{\partial n^2} \frac{\partial^2 w}{\partial s^2} - \left(\frac{\partial^2 w}{\partial n \partial s} \right)^2 \right] \right\},\tag{5}$$

and the component of the energy flux vector in the n-direction is [1]

$$F_n = -V_n \frac{\partial w}{\partial t} + M_n \frac{\partial^2 w}{\partial n \, \partial t},\tag{6}$$

or, using the previous definitions,

$$\frac{F_n}{D} = \frac{\partial w}{\partial t} \left[\frac{\partial}{\partial n} \left(\frac{\partial^2 w}{\partial n^2} + v \frac{\partial^2 w}{\partial s^2} \right) + 2(1 - v) \frac{\partial}{\partial s} \frac{\partial^2 w}{\partial n \partial s} \right] - \frac{\partial^2 w}{\partial n \partial t} \left(\frac{\partial^2 w}{\partial n^2} + v \frac{\partial^2 w}{\partial s^2} \right). \tag{7}$$

Applying the conservation relation (4) to a simply connected area A, with boundary C and outward normal \mathbf{n} , gives

$$\frac{\partial}{\partial t} \int_{A} U \, \mathrm{d}A + \int_{C} F_{n} \, \mathrm{d}s = 0. \tag{8}$$

The boundary integral can be simplified by rewriting equation (7) as

$$F_n = \hat{F}_n + D(1 - v) \left[\frac{\partial^2 w}{\partial n \partial t} \frac{\partial^2 w}{\partial s^2} + 2 \frac{\partial w}{\partial t} \frac{\partial}{\partial s} \frac{\partial^2 w}{\partial n \partial s} - \frac{\partial w}{\partial t} \frac{\partial}{\partial n} \frac{\partial^2 w}{\partial s^2} \right], \tag{9}$$

where

$$\hat{F}_n \equiv D \left(\frac{\partial w}{\partial t} \frac{\partial}{\partial n} \Delta w - \frac{\partial^2 w}{\partial n \partial t} \Delta w \right). \tag{10}$$

Integrating by parts with respect to s, equation (8) reduces to

$$\frac{\partial}{\partial t} \left\{ \int_{A} U \, \mathrm{d}A + D(1 - v) \int_{C} \frac{\partial w}{\partial n} \frac{\partial^{2} w}{\partial s^{2}} \, \mathrm{d}s \right\} + \int_{C} \hat{F}_{n} \, \mathrm{d}s = 0. \tag{11}$$

We now assume that the motion is periodic and define the time average of a physical quantity f over one period as $\langle f \rangle$. Averaging the energy conservation relation (8) implies that the surface integral of the flux $\langle F_n \rangle$ vanishes for any contour not enclosing sources. However, according to equation (11), the same is true of the "simplified" flux $\langle \hat{F}_n \rangle$. Thus, although $\hat{\mathbf{F}}$ is not the instantaneous flux, its time average coincides with the time average of the true flux. The simpler form of $\hat{\mathbf{F}}$ makes it more suitable for using in practice to check the conservation of energy. To be specific, we consider time harmonic motion of the form $w(\mathbf{x}, t) = \text{Re} [W(\mathbf{x}) e^{-i\omega t}]$, for which the energy conservation relation is

$$\int_{C} \langle F_{n} \rangle \, \mathrm{d}s = \int_{C} \langle \hat{F}_{n} \rangle \, \mathrm{d}s = \omega \, \frac{D}{2} \, \mathrm{Im} \int_{C} \left(W \, \frac{\partial}{\partial n} \, \Delta W^{*} - \Delta W^{*} \, \frac{\partial W}{\partial n} \right) \mathrm{d}s = 0, \tag{12}$$

where we have used the definition of \hat{F}_n in equation (10).

The identity (12) for W can be derived more directly as follows. The time harmonic version of equation (3) is

$$\Delta^2 W - k^4 W = Q/D, \tag{13}$$

where $k^4 = \omega^2 \rho h/D$, and Q is the fourier transform of q. Let W^* denote the complex conjugate of W. It may be easily checked, using integration by parts, that

$$\int_{A} W(\Delta^{2}W^{*} - k^{4}W^{*}) dA = \int_{A} (|\nabla W|^{2} - k^{4}|W|^{2}) dA$$
should be \Delta
$$+ \int_{C} \left(W \frac{\partial}{\partial n} \Delta W^{*} - \Delta W^{*} \frac{\partial W}{\partial n} \right) ds = 0. \quad (14)$$

Hence, taking the imaginary part of this identity yields equation (12). Although this derivation is simpler and more direct, it does not show how the integral is related to the energy flux conservation. Nor is it apparent that the flux relation applies to arbitrary periodic motion, as opposed to time harmonic motion.

2.3. AN OPTICAL THEOREM FOR FLEXURAL WAVES

Now consider a finite region of an otherwise homogeneous plate of infinite extent which contains a *scatterer*, which is by definition some type of obstacle that causes scattering of incident waves. It may consist of a region with different plate properties (thickness, density, etc.) or it could be an attachment of some type. In any event, the identity (12) applies to the flux generated by the *total* field, but it does not apply to the flux defined by the scattered part of the response, $W^{sc} = W - W^{inc}$, where W^{inc} is the incident wave, which we assume

to be a straight-crested wave. The scattered far field amplitude $f(\theta)$ is defined such that

$$W^{sc} = \frac{1}{\sqrt{2r}} e^{i(kr - \pi/4)} f(\theta) + o(1/\sqrt{r}), \qquad r \to \infty.$$
 (15)

The average energy flux of the incident wave $W^{inc} = e^{ikx} = e^{ikr\cos\theta}$ across a unit length of any wavefront, x being constant, is simply $\omega k^3 D$, and the energy flux associated with the scattered field follows by substituting from equation (15) into equation (12) while letting the contour C recede to infinity. The *scattering cross-section*, σ^{sc} , defined as the ratio of the latter flux to the incident flux, is therefore

$$\sigma^{sc} = \frac{1}{2} \int_0^{2\pi} |f(\theta)|^2 d\theta.$$
 (16)

Note that σ^{sc} has dimensions of length. Assuming that the scatterer does not use up, or dissipate, energy, we may apply the energy flux equation (12). Thus, substitute for the total field in equation (12) using the incident wave and the far field scattered response, and again let the contour tend to infinity. The flux across C associated with the incident wave vanishes, while the remaining terms give

$$\int_{0}^{2\pi} |f(\theta)|^{2} d\theta + \lim_{r \to \infty} \sqrt{2r} \operatorname{Re} \left\{ e^{-i\pi/4} \int_{0}^{2\pi} (1 + \cos \theta) e^{ikr(1 - \cos \theta)} f(\theta) d\theta \right\} = 0.$$
 (17)

The limit can be evaluated by first approximating the integral asymptotically using the method of stationary phase and then taking the limit to yield, using equation (16),

$$\sigma^{sc} = -2\sqrt{\frac{\pi}{k}} \operatorname{Re} f(0). \tag{18}$$

This is an expression of energy conservation which is related to the optical theorem of classical acoustics and electromagnetics [9, 10]. The optical theorem has been applied to 2-D scattering [12] and has been generalized to include scattering from baffled flexible surfaces [11], but as far as we know it has not been previously derived or used in the context of flexural wave scattering. The energy flux identity (12) is different than the corresponding relation for acoustics, which does not involve the Laplacian operator. However, the final expression of the optical theorem, equation (18), is identical to the analogous 2-D acoustic equation. The reason for this is clear, *a posteriori* at least. The "interior" scattering process is governed by the flexural wave equation (13). However, both the incident straight-crested wave and the far field are solutions to the acoustic Helmholtz equation, and it is this equation which determines the energy conservation equation (18).

The scattered flexural displacement can always be expanded in a set of complete wave functions. Thus, the general form of the scattered field can be represented as [2]

$$W^{sc} = \sum_{n=0}^{\infty} \mathbf{H}_n^{(1)}(kr)(A_n \cos n\theta + A_n' \sin n\theta) + \sum_{n=0}^{\infty} \mathbf{K}_n(kr)(B_n \cos n\theta + B_n' \sin n\theta), \quad (19)$$

where $A'_0 = B'_0 = 0$. This type of representation is appropriate for scatterers of circular shape, and will be used in the next section. Equation (19) may be also used for arbitrary scattering configurations, although other basis functions might be appropriate if the geometry is separable, such as for elliptical regions [2]. The far field amplitude follows from the definition in equation (15) and the asymptotic behavior of Hankel functions:

$$f(\theta) = \frac{2}{\sqrt{\pi k}} \sum_{n=0}^{\infty} (-i)^n (A_n \cos n\theta + A'_n \sin n\theta).$$
 (20)

Hence, equation (16) and the optical theorem (18) imply the identity

$$|A_0|^2 + \operatorname{Re} A_0 + \sum_{n=1}^{\infty} \{ |A_n|^2 / 2 + |A'_n|^2 / 2 + \operatorname{Re} [(-i)^n A_n] \} = 0.$$
 (21)

This serves as a numerical check on any computed results, and will be used in the examples discussed next.

3. SCATTERING BY A CYLINDRICAL INHOMOGENEITY

3.1. GENERAL SOLUTION

We consider a circular region of inhomogeneity in $r \le a$, which is perfectly bonded to the exterior region along the boundary r = a. Let the exterior, infinite plate be denoted by 1, and the scatterer by 2, so that the properties in each region are D_j , v_j , ρ_j and h_i , j = 1, 2. We consider time harmonic motion, so the wavenumbers are k_1 and k_2 . For simplicity, we take the incident wave in the x-direction, or $\theta = 0$, so that $A'_n = B'_n = 0$ in equation (19). The total displacement is of the form

$$W = \begin{cases} e^{ik_{1}r\cos\theta} + \sum_{n=0}^{\infty} \left[A_{n} H_{n}^{(1)}(k_{1}r) + B_{n} K_{n}(k_{1}r) \right] \cos n\theta, & r > a, \\ \sum_{n=0}^{\infty} \left[C_{n} J_{n}(k_{2}r) + D_{n} I_{n}(k_{2}r) \right] \cos n\theta, & r \leqslant a. \end{cases}$$
(22)

The choice of the wave functions is dictated by the conditions that the scattered response is finite at r=0 and must be outgoing, or radiating, as $r\to\infty$. There are four continuity conditions on r=a, requiring that W, $\partial W/\partial r$, M_r and V_r are continuous across the boundary. We note that $e^{ik_1r\cos\theta} = \sum_{m=0}^{\infty} \epsilon_n i^n J_n(k_1r)$, where $\epsilon_0 = 1$, $\epsilon_n = 2$ and $n \ge 1$, and also that the quantities defined in equations (1) and (2) become, in cylindrical co-ordinates [1],

$$M_r = -D \left[\frac{\partial^2 w}{\partial r^2} + v \left(\frac{1}{r} \frac{\partial w}{\partial r} + \frac{1}{r^2} \frac{\partial^2 w}{\partial \theta^2} \right) \right], \tag{23a}$$

$$V_r = -D\frac{\partial}{\partial r}\Delta w - D(1-v)\frac{1}{r^2}\frac{\partial}{\partial \theta}\left(\frac{\partial^2 w}{\partial r\partial\theta} - \frac{1}{r}\frac{\partial w}{\partial\theta}\right),\tag{23b}$$

Applying the continuity conditions for each azimuthal order n = 0, 1, 2, ..., we arrive at the following set of equations for the unknowns:

$$\begin{bmatrix} H_{n}^{(1)}(\kappa_{1}) & K_{n}(\kappa_{1}) & -J_{n}(\kappa_{2}) & -I_{n}(\kappa_{2}) \\ \kappa_{1}H_{n}^{(1)'}(\kappa_{1}) & \kappa_{1}K_{n}'(\kappa_{1}) & -\kappa_{2}J_{n}'(\kappa_{2}) & -\kappa_{2}I_{n}'(\kappa_{2}) \\ S_{H}(\kappa_{1}) & S_{K}(\kappa_{1}) & -S_{J}(\kappa_{2}) & -S_{I}(\kappa_{2}) \\ T_{H}(\kappa_{1}) & T_{K}(\kappa_{1}) & -T_{J}(\kappa_{2}) & -T_{I}(\kappa_{2}) \end{bmatrix} \begin{bmatrix} A_{n} \\ B_{n} \\ C_{n} \\ D_{n} \end{bmatrix} = -\epsilon_{n}i^{n} \begin{bmatrix} J_{n}(\kappa_{1}) \\ \kappa_{1}J_{n}'(\kappa_{1}) \\ S_{J}(\kappa_{1}) \\ T_{J}(\kappa_{1}) \end{bmatrix}. (24)$$

The following notation is used:

$$S_X(\kappa_\alpha) = D_\alpha [n^2(1 - \nu_\alpha) \mp \kappa_\alpha^2] X_n(\kappa_\alpha) - D_\alpha (1 - \nu_\alpha) \kappa_\alpha X_n'(\kappa_\alpha), \tag{25a}$$

$$T_X(\kappa_\alpha) = D_\alpha [n^2(1 - \nu_\alpha)] \mathbf{X}_n(\kappa_\alpha) - D_\alpha [n^2(1 - \nu_\alpha) \pm \kappa_\alpha^2] \kappa_\alpha \mathbf{X}_n'(\kappa_\alpha), \tag{25b}$$

for $\alpha = 1, 2$, where $\kappa_{\alpha} = k_{\alpha}a$, and the upper (lower) signs refer to $X = H^{(1)}$, J, (I, K), respectively. The second order ODEs for these functions have been used to simplify S_X and T_X .

3.2. RIGID AND SOFT LIMITS

There are two limits of interest, corresponding to the limits in which the heterogeneity is either rigid or soft. The former corresponds to clamped conditions at r = a, while the soft limit gives a hole in r < a. In either case, only the field for $r \ge a$ is meaningful in equation (22), and the matrix system (24) reduces to a 2×2 system. For the rigid limit, the matrix comes from the upper left block in equation (24), and gives (dropping the subscript 1 as redundant)

$$A_{n} = -\epsilon_{n} i^{n} \left[\frac{J_{n}(ka) K'_{n}(ka) - J'_{n}(ka) K_{n}(ka)}{H_{n}^{(1)}(ka) K'_{n}(ka) - H_{n}^{(1)'}(ka) K_{n}(ka)} \right],$$
(26a)

$$B_n = \epsilon_n \frac{2i^{n+1}}{\pi ka} \left[H_n^{(1)}(ka) K_n'(ka) - H_n^{(1)'}(ka) K_n(ka) \right]^{-1}, \tag{26b}$$

where the expression for B_n has been simplified using the Wronskian relation for Bessel functions [13]. The matrix for the case of a circular hole corresponds to the lower left block in equation (24), and yields

$$A_n = -\epsilon_n i^n \left[\frac{S_J(ka) T_K(ka) - T_J(ka) S_K(ka)}{S_H(ka) T_K(ka) - T_H(ka) S_K(ka)} \right], \tag{27a}$$

$$B_{n} = -\epsilon_{n} i^{n} \left[\frac{T_{J}(ka) S_{H}(ka) - S_{J}(ka) T_{H}(ka)}{S_{H}(ka) T_{K}(ka) - T_{H}(ka) S_{K}(ka)} \right].$$
 (27b)

It can be checked by asymptotic expansions that in the low frequency limit, $ka \rightarrow 0$, all of the coefficients A_n tend to zero for the rigid case, except A_0 , which tends to -1. This low frequency behavior of the rigid inclusion can be understood by considering the limit of a fixed point at r = 0, i.e., such that the origin is constrained not to move. Consider the point force Green function, W^G , which solves equation (13) with $Q/D = \delta(\mathbf{x})$. It can be shown that [3]

$$W^{G}(\mathbf{x}) = \frac{\mathrm{i}}{8Dk^{2}} \left[\mathbf{H}_{0}^{(1)}(kr) - \mathbf{H}_{0}^{(1)}(ikr) \right], \tag{28}$$

where $H_0^{(1)}(ikr) = (-2i/\pi)K_0(kr)$ [13]. We assume that the scattering from the constrained point is of the form $W^{sc} = F_0W^G$. Then using the fact that $W^G(0) = i(8Dk^2)^{-1}$, we find that the force required to make the total displacement vanish at the origin, W(0) = 0, is $F_0 = i(8Dk^2)^{-1}$. The scattered far field is therefore defined by equation (20) with $A_0 = -1$, and $A_n = B_n = 0$, $n \ge 1$, or $f(\theta) = -2/\sqrt{\pi k}$. The scattering cross-section follows from equation (16) or equation (18) as

$$\sigma^{sc} = 4/k$$
, fixed point at $r = 0$. (29)

Thus, the scattering cross-section increases without bound as the frequency tends to zero. The appearance of the equivalent force F_0 appears to invalidate the flux analysis, and the flux relation (18), among others. However, the equivalent force does no work and hence introduces no extra energy into the system.

The low frequency response of the rigid obstacle is in sharp contrast to the corresponding limit for the hole, for which

$$A_{0} = i \frac{\pi}{4} \frac{v}{1 - v} (ka)^{2} + O((ka)^{3}), \qquad A_{1} = \pi(ka)^{4} + O((ka)^{5}),$$

$$A_{2} = -i \frac{\pi}{4} \frac{1 - v}{1 + v} (ka)^{2} + O((ka)^{3}), \qquad A_{n} = o((ka)^{2}), \quad n = 3, 4, \dots$$
(30)

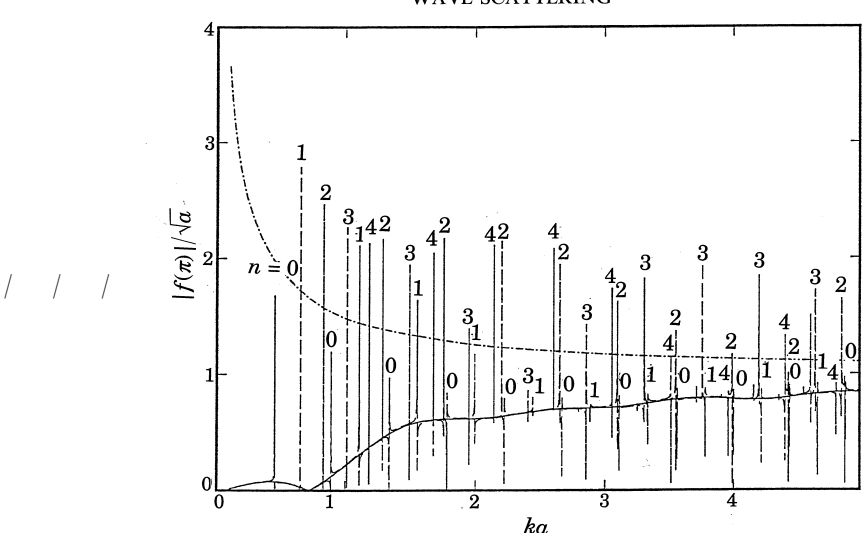


Figure 1. The magnitude of the backscattered far field flexural response for an incident wave of unit amplitude. The surrounding plate is steel of thickness 1 in. Three curves are shown: ——, the limiting case of a hole, ———, a rigid inclusion; ——, an inclusion of the same material but of a thickness that is 1/50th of the surrounding plate.

These results were obtained from equation (27a) using a symbolic manipulation package. The dominant coefficients are A_0 and A_2 , both of order $(ka)^2$ as $ka \rightarrow 0$. Hence, the scattering pattern at low frequency is dominated by the monopole and quadropole terms:

$$f(\theta) \approx \frac{\mathrm{i}}{2} \sqrt{\frac{\pi}{k}} \left[\frac{v}{1-v} + \frac{1-v}{1+v} \cos 2\theta \right] (ka)^2, \quad \text{hole, } ka \to 0.$$
 (31)

This implies that the cross-section vanishes like

$$\sigma^{sc} = \frac{\pi^2}{4} \left[\left(\frac{v}{1 - v} \right)^2 + \frac{1}{2} \left(\frac{1 - v}{1 + v} \right)^2 \right] k^3 a^4, \quad \text{hole, } ka \to 0.$$
 (32)

These results are, perhaps, not that surprising. At long wavelengths the hole becomes "invisible" to an incident wave, but the rigid region has an influence even as the wavelength

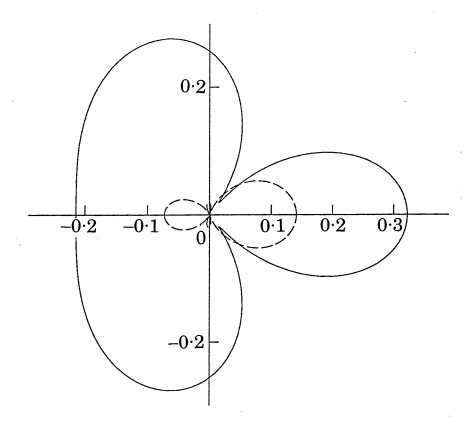


Figure 2. A polar plot of the far field scattering amplitude for a circular hole in a 1 in steel plate. Two different frequencies are shown: ---, ka = 1; ---, ka = 0.5. The wave is incident from the left.

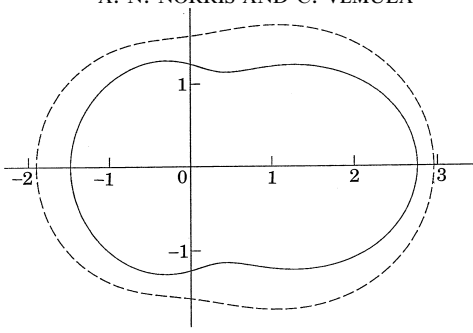


Figure 3. As Figure 2 but for a rigid inclusion of the same extent. —, ka = 1; —, ka = 0.5.

becomes infinite in comparison with its dimension. However, it is interesting to note that the rigid obstacle behaves as a monopole, while the hole is a combination of a monopole (n = 0) and a quadropole (n = 2).

The backscattered fields for both the rigid and soft limits are plotted versus ka in Figure 1, which contains additional curves discussed below. As expected, we note that in the low frequency limit the backscatterer goes to zero for a hole and increases without bound for a rigid inhomogeneity. In the high frequency limit, the backscatter asymptotically approaches unity for both the hole and rigid inhomogeneities. This may be explained on the basis of the reflection from a flat interface, modified by a geometrical correction due to the curvature of the interface. The asymptotic value of the backscatter is unity, because the reflection coefficient for either a rigid or a free edge is of unit amplitude. In Figures 2–4 are shown polar plots of the far field scattering amplitude ($|f(\theta)|$) for the hole and rigid inhomogeneities. We note from Figures 2 and 3 that as the frequency is reduced, $|f(\theta)|$ decreases for the hole and increases for the rigid inhomogeneity. Note from Figure 2 that the hole displays a characteristic "figure of eight" scattering pattern at low frequency. The scattering is mainly in the forward and backward directions, with very little side scattering. This is consistent with the monopole plus quadropole form of the far field amplitude in equation (31). On the other hand, the directionality of the scattered field is lost for the rigid inhomogeneity as ka decreases, in keeping with the above finding that the rigid inclusion behaves like a monopole in the low frequency limit. In the high frequency limit, the scattered field is of the same order of magnitude for both the hole and rigid inhomogeneities, and strong directional scattering is also exhibited in both cases. The large forward lobes in Figure 4 indicate a shadowing effect which becomes stronger with increasing frequency. The scattered response essentially cancels the incident wave in the shadow region.

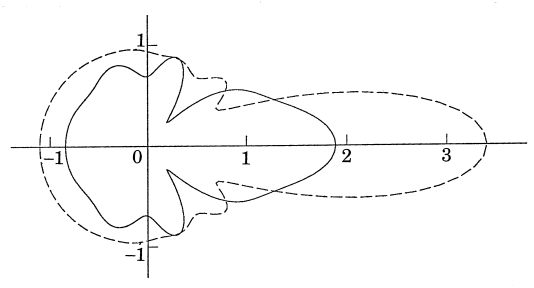


Figure 4. Polar plots of the far field amplitude for both a hole (---) and a rigid inclusion (---) of the same size at ka = 5. Note the appearance of shadow lobes, particularly for the rigid obstacle.



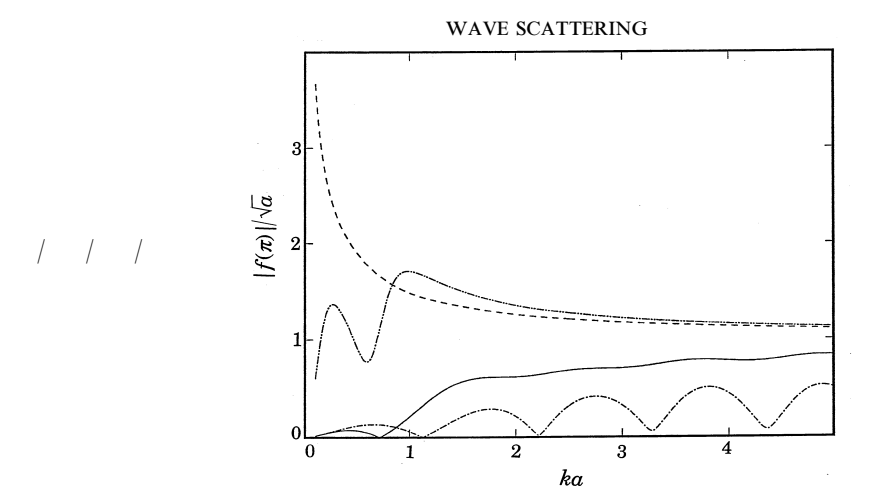


Figure 5. These curves are as in Figure 1: ——, the limiting case of a hole; ——, a rigid inclusion; ——, a bonded steel inclusion of thickness 0.5 in; ——, a heavy, bonded inclusion with the elastic properties of steel and mass equivalent to a plate of thickness 50 in. This was chosen to demonstrate the tendency towards the rigid obstacle limit as the inclusion mass increases. Note that while the curve does approximate the curve for the rigid case at ka > 1, it still tends to zero as $ka \to 0$, as one would expect for a non-rigid obstacle.

3.3. COMPARISONS WITH THE GENERAL CASE

The general case, for which the 4×4 matrices are used to find the unknowns A_n , B_n , C_n and D_n , simulates the soft and rigid limits when the thickness of the inhomogeneous material tends to zero and to infinity, respectively. In Figures 1 and 5, we have considered three cases representative of a "typical" inclusion, a "membrane" type inclusion approximating a hole, and a massive inclusion approximating a rigid obstacle. These are modelled as equivalent plates with the same properties as the surrounding 1 in thick steel plate but with thicknesses of 1/2 in, 1/50 in and 50 in, respectively. As the thickness of the inhomogeneous material is reduced, the backscattered field approaches the backscattered field of the soft limit, as can be seen in Figure 1. An exceedingly thin plate can be considered as a membrane, in so far as it offers no bending resistance to the surrounding plate (although it does not support in-plane stresses because we are still using the classical plate theory). It is illustrated in Figure 1 that as the membrane limit is approached, the backscattered field deviates sharply, at certain discrete frequencies, from the backscattered field of a hole of the same dimension. These frequencies are identified as the resonance frequencies of the thin "membrane" inclusion with clamped boundary conditions at r = a. The resonance frequencies can be solved by finding the zeroes of the equations:

$$\begin{vmatrix} \mathbf{J}_n(\kappa_2) & \mathbf{I}_n(\kappa_2) \\ \mathbf{J}'_n(\kappa_2) & \mathbf{I}'_n(\kappa_2) \end{vmatrix} = 0, \qquad n = 0, 1, 2, \dots$$
 (33)

These roots have been tabulated by Leissa [2], based upon earlier studies in the literature. We have marked the peaks in Figure 1 with the order n of the dispersion equation, for $n \le 4$. The reason for their appearance in this limit is because the "membrane" offers very little reaction *except* at these frequencies. We note that similar types of singular response from almost rigid or almost soft scatterers are encountered in acoustic scattering problems [14]. In the other limit, it is indicated in Figure 5 that as the thickness of the inclusion becomes much larger than the thickness of the homogeneous plate the backscattered field approaches the backscattered field of a rigid limit, as expected.

4. CONCLUSIONS

Flexural wave scattering from obstacles can be treated by the same techniques commonly used to consider acoustic and electromagnetic problems. The main complication arises from the form of the wave equation (3), which is of higher order than the standard acoustic wave equation. Evanescent "waves" are possible but they have no effect on far field quantities, which depend only upon the radiated flexural waves. Thus, the flux identity (12) and the optical theorem (18) are similar to the acoustic analogs.

We have presented some elementary results for flexural wave scattering from plate inclusions of circular shape. The two extreme cases of rigid inclusions and holes have been examined and both come out of the general analysis naturally. These results are interesting in their own right, but could be used for practical applications. For instance, an effective attenuation in a plate filled with randomly placed small holes may be estimated by equating the energy lost from the effective attenuation with the energy radiated from each hole. Suppose that there are N holes per unit area on average. Neglecting multiple scattering effects, the imaginary part of the flexural wavenumber for the effective coherent wave acquires a small, positive imaginary part,

$$\alpha \equiv \operatorname{Im} k = (N/2)\sigma^{sc},\tag{34}$$

where σ^{sc} is the scattering cross-section for an isolated hole, and it is assumed for simplicity that the holes are of the same size. Let c be the volume fraction of the holes in the plate, $c = N\pi a^2$; then it follows from equations (32) and (34) that

$$\alpha = ck^3 a^2 \frac{\pi}{8} \left[\left(\frac{v}{1-v} \right)^2 + \frac{1}{2} \left(\frac{1-v}{1+v} \right)^2 \right]. \tag{35}$$

Hence, on the basis of this effect alone, we would expect the attenuation to be proportional to $\omega^{3/2}$.

ACKNOWLEDGMENTS

The work of A. N. Norris was supported by the U.S. Office of Naval Research, and that of C. Vemula partly by Exxon Research and Engineering Co.

REFERENCES

- 1. S. TIMOSHENKO 1940 Theory of Plates and Shells. New York: McGraw-Hill.
- 2. A. W. Leissa 1969 Vibration of Plates, NASA SP-160. Washington, D.C.
- 3. L. Cremer, M. Heckl and E. E. Ungar 1980 Structure-borne Sound. Berlin: Springer-Verlag.
- 4. K. F. Graff 1991 Wave Motion in Elastic Solids. New York: Dover.
- I. Dyer 1960 Journal of the Acoustical Society of America 32, 1290–1297. Moment impedance of plates.
- 6. M. KITAHARA 1985 Boundary Integral Equation Methods in Eigenvalue Problems of Elastodynamics and Thin Plates. Amsterdam: Elsevier.
- 7. A. D. Lapin 1990 *Soviet Physics—Acoustics* **36**, 34–36. Scattering of Lamb waves in a plate from attached resonators.
- 8. Y. LEVIATAN, E. EREZ and M. J. BERAN 1992 *Quarterly Journal of Mechanics and Applied Mathematics* **45**, 499–514. A source-model technique for analysis of flexural wave scattering in a heterogeneous thin plate.
- 9. M. Born and E. Wolf 1964 Principles of Optics. New York: Macmillan.
- A. ISHIMARU 1979 Wave Propagation and Scattering in Random Media, Volume 1. New York: Academic Press.
- 11. G. A. KRIEGSMANN, A. N. Norris and E. L. Reiss 1985 *Journal of Sound and Vibration* **99**, 301–307. An "optical" theorem for acoustic scattering by baffled flexible surfaces.

- 12. A. Boström 1987 Journal of Applied Mechanics 54, 503-508. Elastic wave scattering from an interface crack: antiplane strain.

 13. M. Abramowitz and I. Stegun 1972 *Handbook of Mathematical Functions*. New York: Dover.
- 14. G. A. KRIEGSMANN, E. L. REISS and A. N. NORRIS 1985 Wave Motion 6, 501-516. Scattering by penetrable acoustic targets.